

# Photo-induced voltage characteristics of $\text{La}_{0.9}\text{Sr}_{0.1}\text{MnO}_3$ films epitaxially grown on vicinal $\text{SrTiO}_3$ (0 0 1) substrates

Kun Zhao<sup>1,3,4</sup>, Meng He<sup>2</sup>, Guo Zhen Liu<sup>2</sup> and Hui Bin Lu<sup>2</sup>

<sup>1</sup> Department of Mathematics and Physics, China University of Petroleum, Beijing 102249, People's Republic of China

<sup>2</sup> Beijing National Laboratory for Condensed Matter Physics, Institute of Physics, Chinese Academy of Sciences, Beijing 100080, People's Republic of China

<sup>3</sup> International Center for Materials Physics, Chinese Academy of Sciences, Shenyang 110016, People's Republic of China

E-mail: zhk@cup.edu.cn

Received 23 April 2007, in final form 20 July 2007

Published 30 August 2007

Online at [stacks.iop.org/JPhysD/40/5703](http://stacks.iop.org/JPhysD/40/5703)

## Abstract

Transient photo-induced voltage characteristics have been studied in  $\text{La}_{0.9}\text{Sr}_{0.1}\text{MnO}_3$  films on vicinal cut  $\text{SrTiO}_3$  (0 0 1) substrates. The as-received thin films are epitaxially grown on the substrates and predominated by a single (1 0 1)-oriented growth. Under irradiation of a 308 nm laser pulse the voltage signal is pulsed and the response time agrees with the laser pulse width. The dependence of the voltage peak on the tilting angles from  $0^\circ$  to  $45^\circ$  is further measured. For the  $c$ -axis tilt angle, the largest signal does not appear at  $45^\circ$  and the optimum choice is  $\sim 30^\circ$ .

(Some figures in this article are in colour only in the electronic version)

## 1. Introduction

Manganites with the perovskite-type structure ( $\text{ABO}_3$ ) have attracted a great deal of interest because of the versatile electronic states that can be controlled by various kinds of external perturbations [1, 2]. Photoexcitation offers an attractive method to vary the concentration of charge carriers without the added complication of a change in the chemical composition and the crystal structure. Technological interest has centred on bolometers [3, 4], while more basic issues have involved quasi-particle generation and carrier relaxation times [5–9].

A pulsed laser-induced voltage was discovered in epitaxially grown  $\text{La}_{1-x}\text{Ca}_x\text{MnO}_3$  thin films on a vicinal cut substrate [10, 11], and an atomic layer thermopile model based on the existence of off-diagonal elements of the Seebeck tensor was put forward to explain the effect [12–17]. In particular, an ultrafast optical response effect was observed in manganite oxide films under the irradiation of a laser pulse of 25 ps duration, and the rise time is  $\sim 300$  ps [18]. It is noted that no voltage has been found when the photon energy is lower than

the band gap of the manganite [18]. These results reveal that the observed photo-induced voltage signal is a combination of photo-inducing carriers and the Seebeck effect found in a lateral electrical field.

Heating the surface of a manganite thin film by absorption of radiation establishes a temperature gradient  $\nabla T$  perpendicular to the film surface. Due to the Seebeck effect, a thermoelectric field,  $E = S \cdot \nabla T$ , is generated with the Seebeck tensor  $S$  [12]. The lateral voltage can be written as

$$V_l = l(S_{ab} - S_c) \sin(2\theta) \Delta T / 2d. \quad (1)$$

Here  $l$  is the irradiated length by the laser beam between two electrodes,  $S_{ab}$  and  $S_c$  the Seebeck coefficients of the crystalline  $ab$  plane and along the  $c$  axis, respectively,  $\theta$  the tilting angle between the  $c$  axis and the film surface normal  $\vec{n}$  (also the direction of laser irradiation),  $\Delta T$  the temperature difference between the front and back surfaces of the film and  $d$  the film thickness.

We have shown the linear dependence of  $V_l$  on  $\sin(2\theta)$  for small tilting angles from  $0^\circ$  to  $20^\circ$  [18]. However, as we know, equation (1) has not been further probed at a large angle ( $\theta > 20^\circ$ ) due to the difficulty in growing high crystalline quality thin films at vicinal substrates with large miscut angles.

<sup>4</sup> Author to whom any correspondence should be addressed.

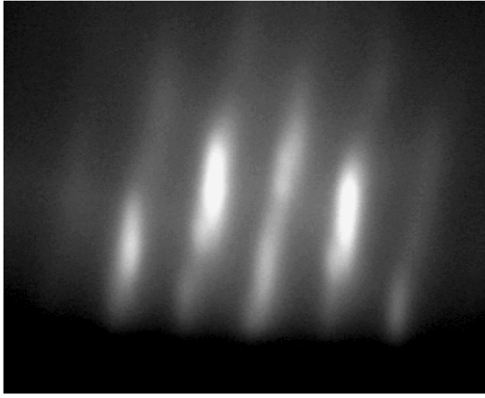


**Figure 1.** RHEED pattern of a LSMO film on the STO (001) substrate with  $10^\circ$  tilting angle.

$\text{La}_{0.9}\text{Sr}_{0.1}\text{MnO}_3$  (LSMO) has a distorted perovskite structure exhibiting an orthorhombic variant. Six possible growth orientations are expected theoretically when the LSMO film epitaxially grows on  $\text{SrTiO}_3$  (STO) (001) [19]. When there is a miscut on the substrate surface, the fourfold symmetry of (001) is broken by exposing the (100) planes at the surface steps, leading to only a single (101)-oriented domain in LSMO films on vicinal STO (001) substrates ( $\theta$  can be as large as  $30^\circ$ ) as displayed in our previous work [20]. Such a microstructural characteristic offers the possibility of validating equation (1).

In this paper, we focus on the angle dependence of  $V_l$  from  $0^\circ$  to  $45^\circ$ . In contrast to the expected result from equation (1) that the laser-induced voltage reaches the maximum at  $45^\circ$ , our results indicate that the optimum angle is not  $45^\circ$  and the largest signal appears at  $\sim 30^\circ$ .

## 2. Experimental procedure

LSMO films with a thickness of about 300 nm were grown on the STO (001) substrates' vicinal cut with the surface at an angle  $\theta$  varying from  $0^\circ$  to  $45^\circ$  to the (001) plane by laser molecular beam epitaxy [21, 22]. The substrate temperature was kept at  $630^\circ\text{C}$  and the oxygen pressure of  $3 \times 10^{-4}$  Pa was maintained throughout the deposition. An *in situ* reflection high energy electron diffraction (RHEED) system and a charge coupled device (CCD) camera were used to monitor the growth process of the LSMO thin films. As shown in figure 1, the streaky and bright RHEED pattern clearly indicates that the films had a good crystallized structure and smooth surface. Taking the  $c$ -axis diffraction peak of the substrate as an internal standard, the x-ray diffraction (XRD) of the LSMO film on the STO (001) substrate with a miscut angle of  $10^\circ$  is performed. To satisfy Bragg's diffraction geometry, the STO [001] axis was aligned carefully and the offset point  $\omega$  was set as  $10^\circ$ .

For the photo-induced voltage measurements, two in-plane electrodes separated by 4 mm were placed on the surface of the LSMO films as displayed in the inset of figure 4(a) and were always kept in the dark to prevent the generation of any electrical contact photovoltaic effect. The output of a Lambda Physik LEXTRA 200 excimer laser (308 nm in wavelength, 20 ns in duration) was used as the laser source. The irradiation area is  $3 \times 2 \text{ mm}^2$  and

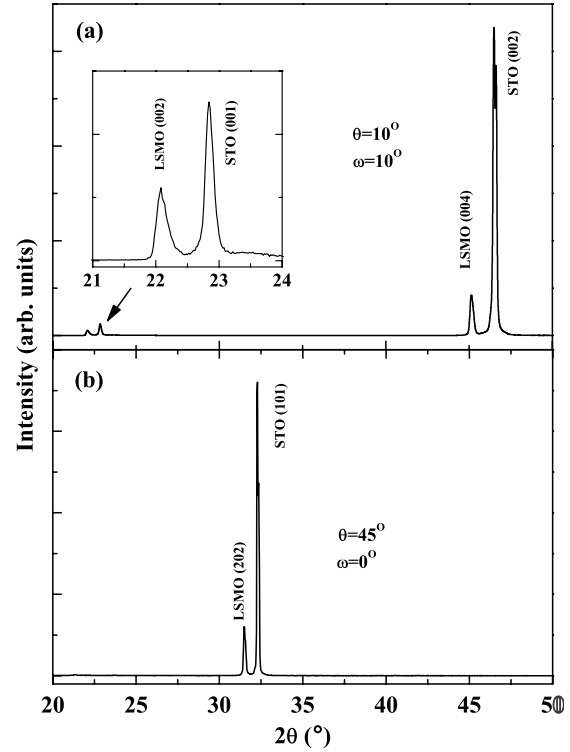


**Figure 2.** XRD patterns of the LSMO thin film with miscut angles of (a)  $10^\circ$  and (b)  $45^\circ$ .

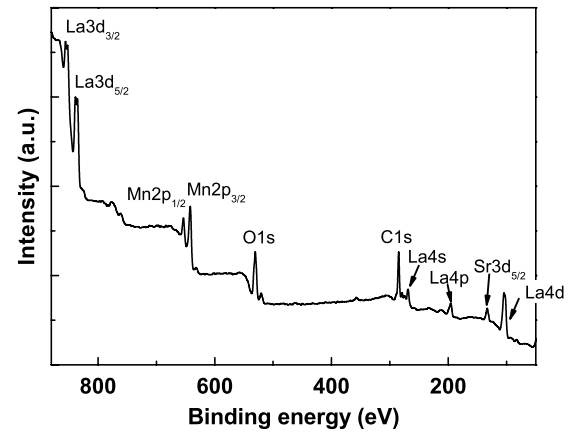


**Figure 3.** XPS pattern of a typical LSMO film at the etching depth of 50 nm.

the signal was monitored with a sampling oscilloscope (500 MHz bandwidth) terminated into  $50 \Omega$  at ambient temperature. Detailed measurement procedure can be found in our previous articles [23–28].

Figure 2 shows the XRD spectrum. As expected, only the peaks with the same orientation as the substrate were detected. In figure 2(a), the coherently tilted LSMO film with  $c$ -axis is exactly along the  $c$ -axis of STO and also inclined by  $\theta$  to the surface normal. As for  $\theta = 45^\circ$  ( $\omega = 0^\circ$ ), the LSMO film also shows a single phase structure and (101) orientation is observed (figure 2(b)).

It is noted that the preparation processing was carried out at a lower oxygen pressure and there is no annealing in the presence of oxygen, so the as-prepared samples are

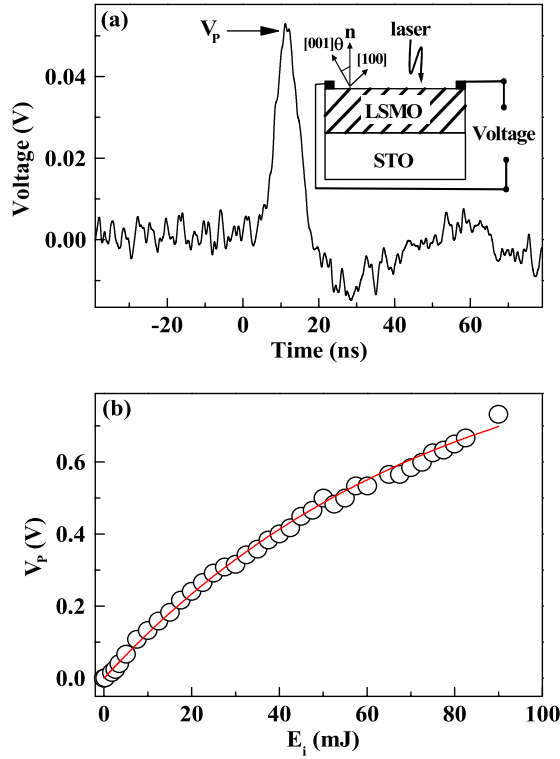


**Figure 4.** (a) A typical optical response consisting of the voltage signal under irradiation of a 308 nm pulsed laser for a duration of 20 ns at room temperature. The tilting angle  $\theta$  is  $10^\circ$  and the on-sample energy is 4.5 mJ. The inset displays the schematic circuit of the optical response measurement.  $V_p$  denotes the peak value of the transient voltage signal. (b) On-sample energy  $E_i$  dependence of  $V_p$ . The solid line is a guide for the eye.

oxygen-deficient. The chemical composition was determined by the x-ray photoelectron spectroscopy (XPS) spectrum at etching depths of 50 nm (figure 3), and the stoichiometry ratio of La, Sr, Mn and O in the LSMO film approached about 0.9 : 0.1 : 1 : 2.7. The oxygen release resulted in the low-angle shift of the LSMO peaks that produced lattice expansion, and similar behaviours have been observed in other deoxidized manganites [29].

Figure 4(a) shows a typical voltage transient of the LSMO thin film on the  $10^\circ$  tilting STO substrate under the irradiation of a pulsed 308 nm laser of 20 ns in duration. The laser energy per pulse is 180 mJ and the on-sample energy is 4.5 mJ. The optical response shows a peak voltage  $V_p$  of  $\sim 0.05$  V and a pulse width of  $\sim 20$  ns in agreement with the laser duration. Figure 4(b) demonstrates the relation between the peak value  $V_p$  and the on-sample energy  $E_i$  for an irradiated area of  $3 \times 2$  mm<sup>2</sup>. We can get  $V_p \propto 1 - \exp(-E_i/E_0)$  by fitting the data carefully ( $E_0 \simeq 75$  mJ). From equation (1), an exponential laser energy density dependence of the temperature gradient  $\nabla T$  is expected.

Theoretically the largest signal will appear at  $\theta = 45^\circ$  ( $\sin(2\theta) = 1$ ). In contrast, the present results as shown in figure 5(a) demonstrate that the detected signal for  $45^\circ$  is basically a random noise due to the electrical-magnetical emission by the operation of the excimer laser. In addition, at  $\theta = 0^\circ$  the peak voltage of  $\sim 0.005$  V departs from equation (1) which gives a zero value for  $\sin(2\theta) = 0$ . Electron diffractions and high-resolution images show an atomically sharp interface

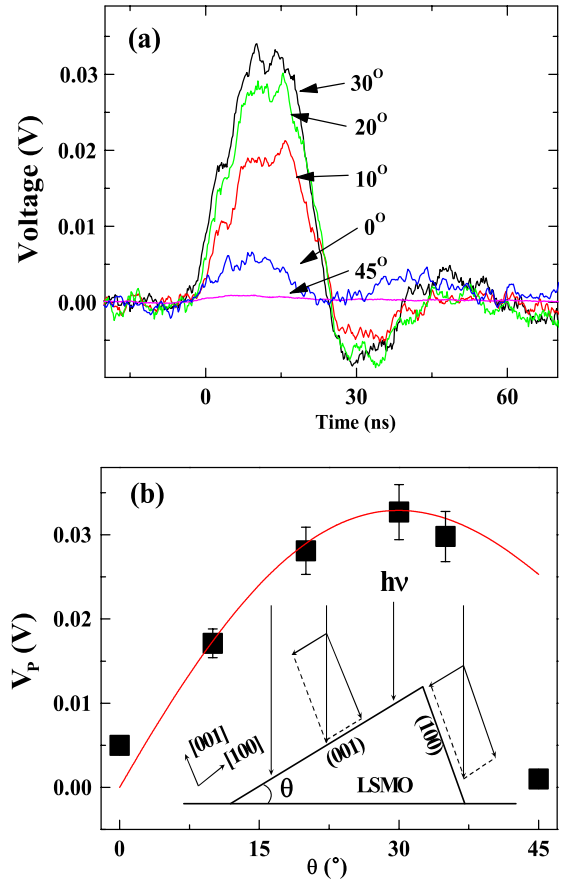


**Figure 5.** (a) Voltage signal as a function of time under 308 nm laser pulses for a duration of 20 ns for different tilting angles. The on-sample energy is about 2 mJ. (b) Dependence of peak voltage  $V_p$  on miscut angle  $\theta$ . The inset shows the schematic drawing under the irradiation of a pulsed laser. The solid line shows the fitting results using equation (3) by inserting  $\alpha = 0.35$ .

of the LSMO film on exact (001) STO ( $\theta = 0^\circ$ ), and the microstructures of as-received LSMO films are clarified in terms of multi-oriented domains forming a rectangular cross-grid pattern [20]. In particular, based on figure 3(a) in our paper [20], the (101) plane of each domain is parallel to the substrate surface, and the boundaries are  $45^\circ$  away from the interface normal [001]. These facts indicate that a photo-induced voltage signal can be detected at  $\theta = 0^\circ$  on the basis of the off-diagonal Seebeck effect as discussed in the  $\text{La}_{0.8}\text{Sr}_{0.2}\text{MnO}_3$  system [30].

Figure 5(b) plots the tilting angle dependence of the peak voltage. The signal amplitude increases with  $\theta$  until  $30^\circ$  and then decreases. It is known that each element of the Seebeck tensor is proportional to the corresponding electrical resistivity of the system. For the present transient process, the transient electrical resistivity along each axis is reverse proportional to the transient carrier density correspondingly. The inset of figure 5(b) shows the schematic drawing under irradiation of a pulsed laser. If the laser beam is divided into two components of being parallel and perpendicular to the tilting direction, the transient carrier density along each axis is proportional to the illuminated power perpendicular to the tilting direction. Thus

$$(S_{[100]} - S_{[001]}) \propto (\rho_{[100]} - \rho_{[001]}) \propto (\alpha \sin \theta - \cos \theta). \quad (2)$$

So, we can get

$$V_l \propto (\alpha \sin \theta - \cos \theta) \sin(2\theta) \Delta T / 2d. \quad (3)$$

The solid line in figure 5(b) shows the calculated result from equation (3) by inserting  $\alpha = 0.35$ .

In contrast to our previous report where the maximum occurs at  $20.9^\circ$  [27], the largest signal in the present results appears at  $\sim 30^\circ$ . This difference can be understood easily. As for the STO single crystal, the resistivity is isotropic, while being anisotropic for LSMO. Thus,  $\alpha = 1$  and  $0.35$  is achieved for STO and LSMO, respectively. Furthermore, the discrepancy at  $45^\circ$  stems from the simplification of the model used in our theory. The study on the true nature behind the transient process of photo-induced voltage is highly expected.

### 3. Summary

In summary, we have investigated the tilting angle dependence of transient photo-induced voltage characteristics of LSMO films epitaxially on vicinal cut STO substrates. The microstructures in the LSMO film on the STO (0 0 1) substrate are clarified in terms of the oriented microdomains, while the films on miscut STO substrates are predominated by a single (1 0 1)-oriented growth. The dependence of the pulsed laser-induced voltage peak on the tilting angles shows that  $45^\circ$  is not the best choice and the largest signal appears at  $\sim 30^\circ$ . The mechanism of such a effect is proposed.

### Acknowledgments

This work has been supported by the National Natural Science Foundation of China (Grant Nos 50672132 and 60576015) and the Key Project of Chinese Ministry of Education (No 107020).

### References

- [1] Kiryukhin V, Casa D, Hill J P, Keimer B, Vigliante A, Tomioka Y and Tokura Y 1997 *Nature* **386** 813
- [2] Asamitsu A, Tomioka Y, Kuwahara H and Tokura Y 1997 *Nature* **388** 50
- [3] Rajeswari R, Chen C H, Goyal A, Kwon C, Robson M C, Ramesh R, Venkatesan T and Lakeou S 1996 *Appl. Phys. Lett.* **68** 3555
- [4] Nikolaenko Yu M, Maksimov I S, Medvedev Yu V, Ulyanov A N and Grishin A M 2000 *Acta Phys. Pol. A* **97** 991
- [5] Zhao Y G, Li J J, Shreekala R, Drew H D, Chen C L, Cao W L and Lee C H 1998 *Phys. Rev. Lett.* **81** 1310
- [6] Averitt R D, Lobad A I, Kwon C, Trugman S A, Thorsmille V K and Taylor A J 2001 *Phys. Rev. Lett.* **87** 017401
- [7] Ogasawara T, Kimura T, Ishikawa T, Kuwata-Gonokami M and Tokura Y 2001 *Phys. Rev. B* **63** 113105
- [8] Dai J M, Song W H, Du J J, Wang J N and Sun Y P 2003 *Phys. Rev. B* **67** 144405
- [9] Zhang R L, Dai J M, Song W H, Ma Y Q, Yang J, Du J J and Sun Y P 2004 *J. Phys.: Condens. Matter* **16** 2245
- [10] Habermeier H U, Li X H, Zhang P X and Leibold B 1999 *Solid State Commun.* **110** 473
- [11] Li X H, Habermeier H U and Zhang P X 2000 *J. Magn. Magn. Mater.* **211** 232
- [12] Lengfellner H, Kremb G, Schnellbögl A, Betz J, Renk K F and Prettl W 1992 *Appl. Phys. Lett.* **60** 501
- [13] Huggard P G, Zeuner S, Goller K, Lengfellner H and Prettl W 1994 *J. Appl. Phys.* **75** 616
- [14] Lengfellner H, Zeuner S and Prettl W 1994 *Europhys. Lett.* **25** 375
- [15] Zeuner S, Prettl W and Lengfellner H 1995 *Appl. Phys. Lett.* **66** 1833
- [16] Zeuner S, Lengfellner H and Prettl W 1995 *Phys. Rev. B* **51** 11903
- [17] Zhang P X, Lee W K and Zhang G Y 2002 *Appl. Phys. Lett.* **81** 4026
- [18] Zhao K, Jin K J, Huang Y H, Lu H B, He M, Chen Z H, Zhou Y L and Yang G Z 2006 *Physica B* **373** 72
- [19] Jiang J C, Tian W, Pan X, Gan Q and Eom C B 1998 *Mater. Sci. Eng. B* **56** 152
- [20] Zhuo M J, Zhu Y L, Ma X L and Lu H B 2006 *Appl. Phys. Lett.* **88** 071905
- [21] Yang G Z, Lu H B, Chen F, Zhao T and Chen Z H 2001 *J. Crystal Growth* **227–228** 929
- [22] Zhao T, Lu H B, Chen F, Dai S Y, Yang G Z and Chen Z H 2000 *J. Cryst. Growth* **212** 451
- [23] Zhao K, Huang Y H, Zhou Q L, Jin K J, Lu H B, He M, Cheng B L, Zhou Y L, Chen Z H and Yang G Z 2005 *Appl. Phys. Lett.* **86** 221917
- [24] Lu H B, Jin K J, Huang Y H, He M, Zhao K, Cheng B L, Chen Z H, Zhou Y L, Dai S Y and Yang G Z 2005 *Appl. Phys. Lett.* **86** 241915
- [25] Huang Y H, Zhao K, Lu H B, Jin K J, Chen Z H, Zhou Y L and Yang G Z 2006 *Appl. Phys. Lett.* **88** 061919
- [26] Zhao K, Jin K J, Lu H B, Huang Y H, Zhou Q L, He M, Chen Z H, Zhou Y L and Yang G Z 2006 *Appl. Phys. Lett.* **88** 141914
- [27] Zhao K, Jin K J, Huang Y H, Zhao S Q, Lu H B, He M, Chen Z H, Zhou Y L and Yang G Z 2006 *Appl. Phys. Lett.* **89** 173507
- [28] Wang X, Xing J, Zhao K, Li J, Huang Y H, Jin K J, He M, Lu H B and Yang G Z 2007 *Physica B* **392** 104
- [29] Sun J R, Yeung C F, Zhao K, Leung C H, Wong H K and Shen B G 2000 *Appl. Phys. Lett.* **76** 1164
- [30] Zhao K, Lu H B, He M, Huang Y H, Jin K J, Chen Z H, Zhou Y L, Yang G Z and Ma X L 2006 *Eur. Phys. J. Appl. Phys.* **35** 173